



# Single nanosecond-pulse production of polymeric fiber Bragg gratings for biomedical applications

XIN CHENG,  DINUSHA SERANDI GUNAWARDENA, \*  CHI-FUNG JEFF PUN, JULIEN BONEFACINO, AND HWA-YAW TAM

Photonics Research Centre, Department of Electrical Engineering, The Hong Kong Polytechnic University, Kowloon, Hong Kong S.A.R, China

\*[dinusha.gunawardena@polyu.edu.hk](mailto:dinusha.gunawardena@polyu.edu.hk)

**Abstract:** In this study, we present first-time fabrication of FBGs in all ZEONEX-based SMPOFs with a single 25 ns pulse of 248 nm UV irradiation over a 12-month period, which opens up new frontiers in optics and photonics for the effective fabrication of polymer optical fiber Bragg gratings (POFBGs), permitting mass producibility of them. POFBGs were characterized by subjecting them to various physical parameters including temperature and tensile strain. Strain responses of FBGs with similar grating strengths fabricated with 248 nm and 325 nm He-Cd laser irradiations were explored over a year to demonstrate their long-term stability and applicability. Owing to the unique features of the proposed sensing device fabricated by embedding POFBGs in silicone rubber, a good performance in the detection of human heart rate with an amplitude of 4 pm, which is 4 times higher compared to that of silica single mode fiber (SMF) was demonstrated. The response of the sensing device during a human respiration process was also explored where exhalation and inhalation were monitored and distinguished while the breath was held. These revelations signify the importance of ZEONEX-based POFBGs, which allow consistent and effective grating fabrication and are highly promising in the foreseeable future for biomedical applications.

© 2020 Optical Society of America under the terms of the [OSA Open Access Publishing Agreement](#)

## 1. Introduction

In the recent years, fiber Bragg grating (FBG) sensors have been attracting the attention of the research community for their potential applications in assisted surgeries and vital-sign-monitoring [1–5]. In these applications, FBGs in polymer optical fibers (POFs), could play a significant role due to their numerous advantages, such as resistance to breakage, small Young's modulus, and biocompatibility [2,6,7]. Apart from sharing the same merits of conventional silica optical fibers, such as immunity to electromagnetic interference, small size and multiplexing capabilities [8], POFs possess many intrinsic features including high flexibility, non-brittle nature, ease of handling, and high fracture toughness. Among POFs, PMMA-based POFs have gained a wide popularity since a variety of dopants can be added to the fiber core to enhance its photosensitivity. He-Cd laser operating at 325 nm is considered to be the preferred choice for fiber Bragg grating (FBG) inscription in these fibers despite the required long inscription time when compared to inscription using 248 nm excimer laser [9]. This is because PMMA exposed to UV irradiation at wavelengths shorter than 300 nm results in the scission of its main chain and cause degradation in PMMA [10]. In our previous research study [6], we investigated the impact of high UV fluences at 325 nm and 248 nm on the mechanical and sensing properties of POFs for high strain measurements using dynamic mechanical analysis and tensile strain. The findings have highlighted that inscription with 325 nm as well as 248 nm UV sources has minimum impact on PMMA POFs in the elastic regime. Furthermore, the unveiling of FBG inscription in PMMA POF using a single nanosecond pulse of 248 nm excimer laser irradiation has opened up the

exciting possibility of mass producibility of polymer FBGs during the fiber drawing process [11]. However, the high loss of PMMA POFs, particularly doped PMMA POFs which can be as large as 100 dB/m, still remains a complication limiting their usage in many practical applications [12].

The advent of POFBGs based on cycloolefin copolymers (COPs), such as TOPAS grade 8007 [13], 5013 [14,15] and ZEONEX grade 480R [16,17], could revolutionize the biomedical sensing industry due to their much lower fiber attenuation coupled with very low affinity towards water. COPs exhibit good chemical inertness to bases, acids, and many polar solvents, compared to the conventional PMMA based POFs [18], which makes them excellent candidates for biomedical applications which are often conducted in aqueous environments. For instance, in an extremely sensitive surgical procedure such as cochlear implantation, the insertion of the implant solely relies on the manual dexterity and steadiness of the skilled otology surgeons [19]. Therefore, it is of utmost importance that the optical sensor exhibits low stiffness properties and provides precise information on the tip force of the implant during the insertion process without the impact of any other external factor such as humidity. Furthermore, biocompatibility together with long-term stability is also vital for such high precision surgical procedure.

Considering the insights of our previous study, where we have demonstrated the insignificant degradation of the performance of an FBG in PMMA POF in the elastic regime upon 248 nm UV irradiation [6], for the first time to the best of our knowledge, in this study, the stability and performance of FBGs inscribed in all ZEONEX-based SMPOF with 248 nm and 325 nm laser irradiation, are investigated over a time frame of one year to ensure their long-term applicability which is crucial for biomedical applications. A comparative study of the strain properties of FBGs inscribed with 325 nm He-Cd laser and 248 nm excimer laser was also conducted. The significantly lower fiber loss in ZEONEX-based POFs compared to that of PMMA, was well documented by Woyessa *et al.* in their recent work demonstrating a loss of ~3dB/m at 796 nm [17] verify their practical usage.

The ZEONEX SMPOF proposed in this study, has a core size of 9.3  $\mu\text{m}$  and a numerical aperture of 0.12 which are similar to that of a silica SMF at the same wavelength of 1550 nm, which facilitates effective and easy coupling. Easy breakage of silica FBGs resulting in sharp fragments of fiber can be considered as one of the main drawbacks of using these fibers in biomedical applications. In this regard, the considerably lower Young's modulus of ZEONEX-based POFs (2.4 GPa) compared to silica fibers (73 GPa) make them more suited for the aforementioned applications. The low Young's modulus of ZEONEX based POFBGs could also be beneficial for minimally invasive surgeries where certain surgical prosthesis such as cochlear implants are preferred to have a reduced stiffness to enhance the sensitivity. Furthermore, POFBGs can also be successfully incorporated in human vital signs monitoring such as human heart rate and respiratory functions. Hence, the discoveries of this study can be regarded as a vital step towards the development of risk-free, sensitive, resilient and disposable medical sensors. In addition, the extremely short time duration of a mere 25 ns devoted in the FBG inscription process of ZEONEX SMPOFs using 248 nm excimer laser irradiation can promote mass producibility of FBGs during the fiber drawing process, which is an important step towards the realization of low-cost production of FBGs which is of interest to the wider sensing industry.

## 2. ZEONEX SMPOF fabrication procedure

### 2.1. Fabrication of ZEONEX SMPOFs

The ZEONEX-based all-solid-single-mode step-index POFs (SIPOFs) in this study, were fabricated using the 'pull-through' [2] method instead of drilling the fiber preform. The ZEONEX SMPOF composed of a single monomer material, was fabricated using different grades of ZEONEX material, where the core (E48R) has a slightly higher refractive index than that of the cladding (480R). The glass transition temperatures ( $T_g$ ) of the two grades of ZEONEX are ~

138 °C which denotes that the fiber can operate at a higher temperature than that of PMMA. The SMPOF was fabricated in-house at The Hong Kong Polytechnic University.

Figure 1 illustrates the fabrication process of pull through method used in this work, in which the core material, ZEONEX E48R, (A) was melted inside a glass tube and the cladding material, ZEONEX 480R, was melted inside another glass tube where a Teflon wire with a diameter of 0.9 mm was placed at the center. Afterwards, the Teflon wire was removed to form a hole in the cladding preform (B). The entire melting process was conducted inside a vacuum oven under a maximum temperature of 245 °C to remove O<sub>2</sub> and air. The core material was then drawn into a cane (C), with a diameter similar to that of the Teflon wire. The core cane was then inserted inside the cladding to form the complete polymer preform assembly, which was eventually drawn into SMPOF (D) with a diameter of 160  $\mu$ m.

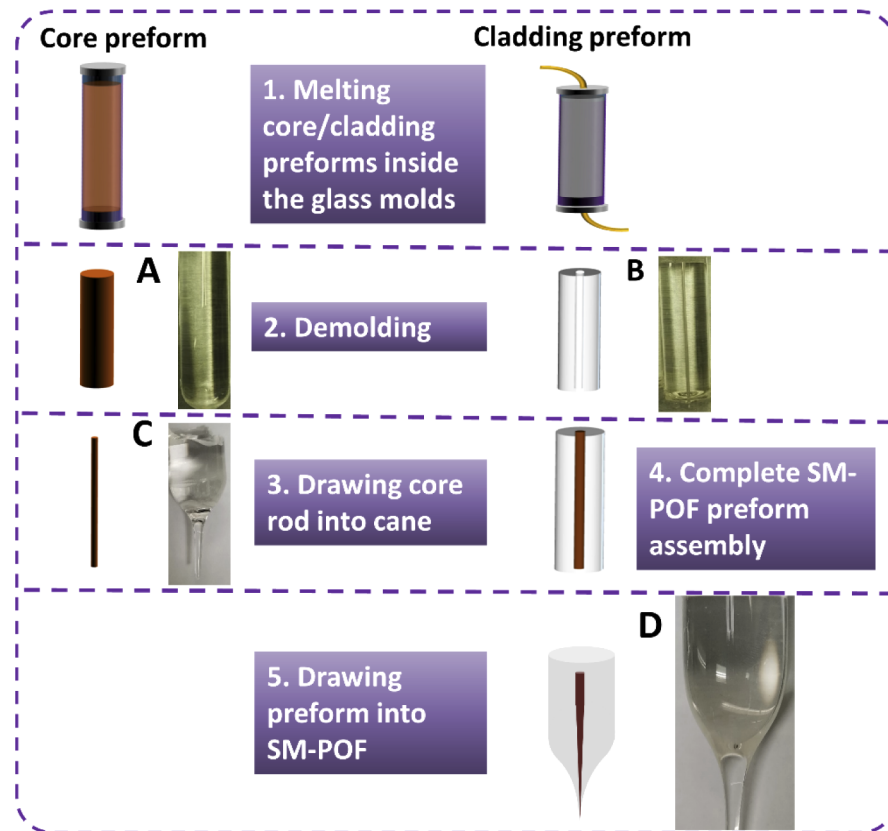


**Fig. 1.** Schematic illustration of ZEONEX SMPOF fabrication procedure following the steps in the order of 1 to 5. Photographs: ZEONEX E48R melted into a cylindrical rod (A); ZEONEX 480R melted into a cylindrical rod with a hole at the center (B); Segment of the cylindrical rod drawn into cane (C); and a segment of the POF preform drawn into SMPOF (D).

Consistent and good quality ZEONEX SMPOFs were fabricated using this technique with a circular core and cladding. Figure 2(a) shows the microscopic image of the fiber cross section of the ZEONEX SMPOF fabricated more than a year ago, and Fig. 2(b) shows the refractive index profile measured by Interfiber Analysis LLC, USA. The core and cladding diameters of the SMPOF are 160  $\mu$ m and 9.3  $\mu$ m, respectively and the refractive index difference between the

core and cladding is 0.0066 which is in excellent agreement with the specification provided by ZEONEX [17].

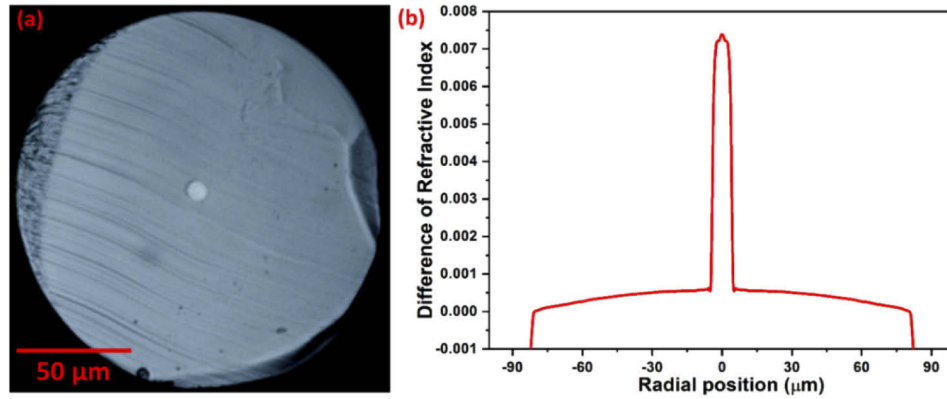


**Fig. 2.** (a) Optical microscopic image of the fiber cross section and (b) refractive index profile of the ZEONEX SMPOF fabricated in May 2019. The refractive index profile was measured by Interfiber Analysis LLC, USA in August 2019.

## 2.2. Influence of oxygen ( $O_2$ ) on ZEONEX

As discussed in the aforementioned section, the preform was fabricated in a vacuum oven which has the capacity of completely removing  $O_2$  under a -0.1 bar vacuum condition. This step is crucial in the fabrication process, since any  $O_2$  present inside the oven can react with both ZEONEX 480R and ZEONEX E48R resulting in oxidation which in turn will degrade the quality

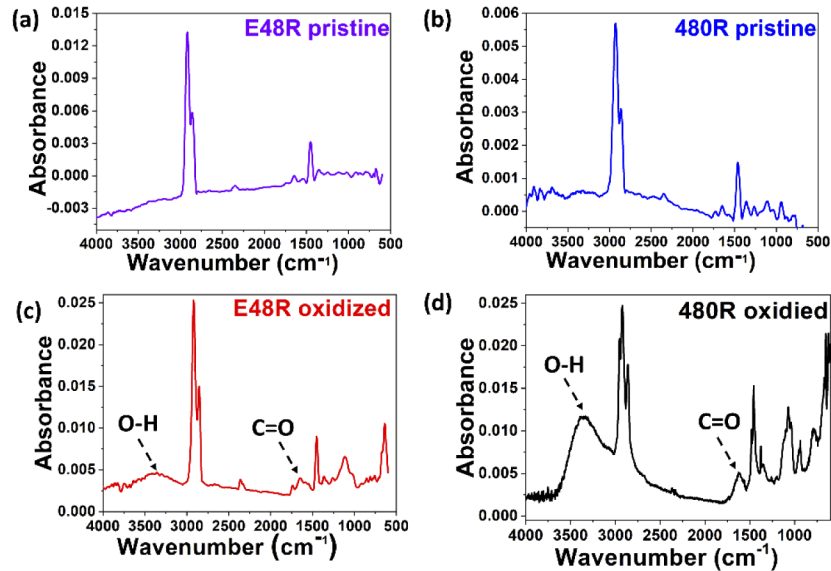


**Fig. 3.** Comparison of FTIR spectra of ZEONEX E48R at (a) pristine and (b) oxidized conditions and ZEONEX 480R at (c) pristine and (d) oxidized conditions. Absorption peaks corresponding to O-H stretch and C=O stretch are observed for both oxidized samples at  $\sim 3400$  and  $1700\text{cm}^{-1}$ , respectively.

of the preform during heating. Reaction of  $O_2$  with these polymer materials can be clearly observed from the Fourier transform infrared spectroscopic (FTIR) measurements shown in Fig. 3. Broad absorption peaks corresponding to an O-H stretch are observed in the region between  $3600$  and  $3100\text{ cm}^{-1}$  for both E48R and 480R samples when heated with  $O_2$  where a maximum absorption occurs at  $3400\text{ cm}^{-1}$  in 480R. The second most important feature of the FTIR spectrum is the presence of a strong signal at  $\sim 1700\text{ cm}^{-1}$  which corresponds to a C=O stretch, signifying the existence of carbonyl or carboxyl groups in both the samples.

### 2.3. Physical properties of SMPOFs

**Tg and stress-strain measurements of SMPOF.** Tg of the fabricated SMPOFs was measured using a differential scanning calorimetry (DSC) machine (METTLER TOLEDO, Model: DSC3). The heat absorption characteristics of an SMPOF sample was analyzed by heating the sample at a ramping rate of  $4\text{ }^\circ\text{C/min}$  over a temperature range from  $100\text{ }^\circ\text{C}$  to  $250\text{ }^\circ\text{C}$  under a constant nitrogen gas flow of  $50\text{ ml/min}$ . Figures 4(a) and (b) show the heat flow of the SMPOF sample during the heating process in the DSC machine. The measured value of Tg is  $137.7\text{ }^\circ\text{C}$  which is as same as that of ZEONEX 480R specified by the manufacturer [18]. This verifies the absence of any chemical reaction during the SMPOF fabrication process. Stress-strain measurements based on dynamic mechanical analysis (DMA) method were performed to characterize the mechanical properties of the SMPOFs. The investigation was carried out using a DMA machine (METTLER TOLEDO, Model: DMA1) on a  $160\text{ }\mu\text{m}$  diameter SMPOF sample.

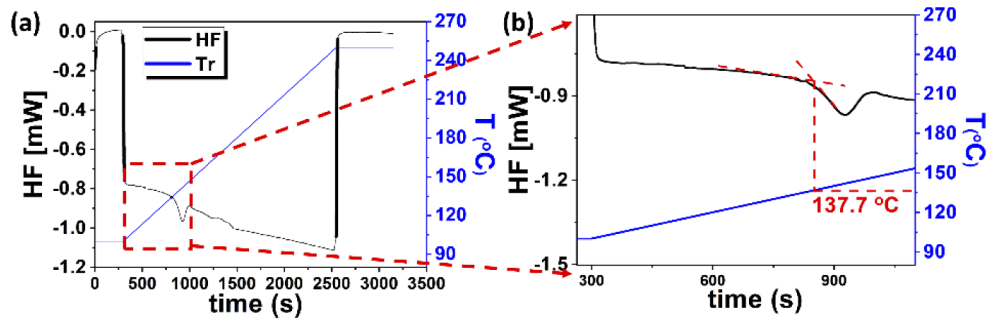


**Fig. 4.** (a) Tg measurement of the fabricated SMPOF and (b) the expanded view of a selected segment of it indicating a measured Tg of  $137.7\text{ }^\circ\text{C}$ .

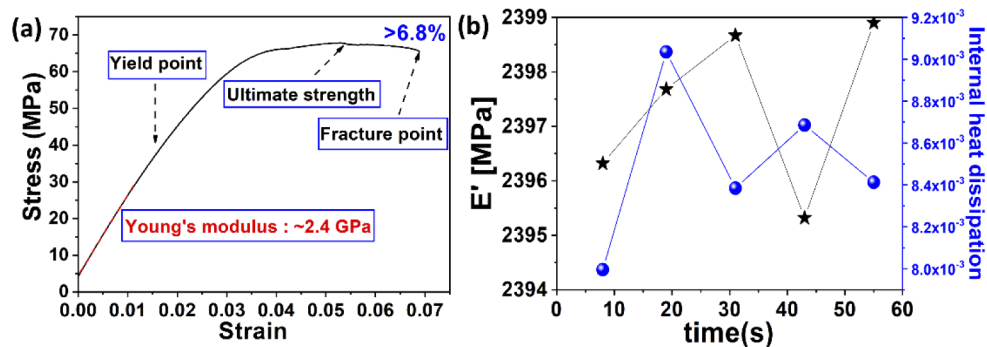


**Fig. 5.** (a) Stress-strain curve and (b) Young's modulus measurements of the fabricated SMPOF with a diameter of  $160\text{ }\mu\text{m}$  and a length of  $1\text{ cm}$ .



Figure 5(a) shows the measured tensile strength of the SMPOF sample and Fig. 5(b) depicts its Young's modulus measurements which are derived from the linear region of the stress-strain curve in Fig. 5(a). The result shows that the average Young's modulus is  $\sim 2.4$  GPa and the elongation-at-break is over 6.8% elongation. From Fig. 5(b), the measured value of internal dissipation, which is  $\sim 8 \times 10^{-3}$  indicates that the energy loss at each measurement point is considerably small. This denotes that, when the SMPOF is subjected to an elongation, the energy transferred from mechanical energy to thermal energy is rather less and hence, results in only a slight temperature change during the Young's modulus measurement.

### 3. Results and discussion

#### 3.1. Temperature and strain responses of FBGs inscribed in SMPOFs

FBG inscriptions were carried out in ZEONEX SMPOF with the aid of a 248 nm KrF excimer laser and 325 nm He-Cd laser more than a year ago to study the long-term impact of UV fluence on ZEONEX POF. The optical fibers were stored under room temperature over the year. In order to investigate the impact of 248 nm irradiation on the physical properties of ZEONEX POFBGs, suitable for biomedical applications of our interest, 2 mm long gratings were fabricated using two pulses of 248 nm laser irradiation, with a pulse energy of 50 mJ.

Subsequently, to ensure the long-term feasibility, the responses of the FBGs to temperature were explored since this parameter plays an important role in a bio-sensing system. In a typical bio-sensing system, the operating temperature is lower than 50 °C and the surrounding environment has a specific relative humidity level. An environmental chamber (R-PTH80L, RUI KAI) was used to investigate the temperature response. The temperature responses of two POFBGs at a fixed humidity level of 50%RH were investigated where the fabrication time of the two FBGs was one year apart, in the same batch of ZEONEX POF which was drawn in May 2019. The Bragg wavelength shift of the FBGs were monitored over a temperature range from 30-70 °C in a stepwise process where the temperature was maintained at each step for a time duration of 30 mins. This testing range complies with the typical temperature measurement range of bio-sensing applications. An interrogator (MOI Si155) with a resolution of 1 pm was used to record the data and the results obtained are shown in Fig. 6 which demonstrates a linear response with temperature sensitivities of  $-24.7$  pm/°C and  $-25.47$  pm/°C for the FBGs fabricated in May 2020 and May 2019, respectively.

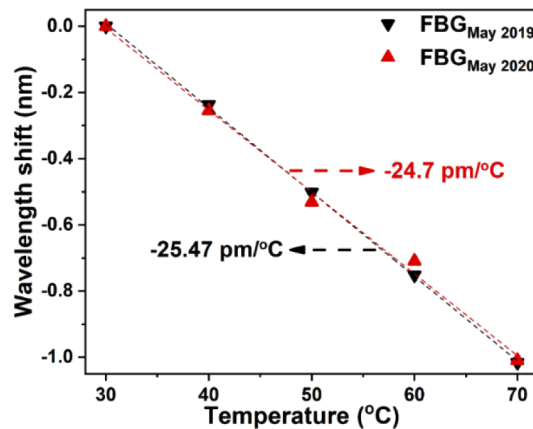


**Fig. 6.** Comparison of temperature responses of ZEONEX POFBGs inscribed within a time span of one year. The black curve denotes the response of the FBG inscribed in May 2019 and the red curve denotes the response of the FBG inscribed in May 2020. Both FBGs were inscribed in the same batch of ZEONEX POF drawn in May 2019.

Strain response of the fabricated SMPOF is a crucial criteria for potential usage in biomedical sensing applications as it is influenced by the very low Young's modulus of such type of fibers, which results in a much higher sensitivity compared to its silica counterparts. Figure 7 shows the strain responses of the FBGs fabricated within a time duration of one year. Commendable repeatability with strain sensitivities of  $\sim 1.6$  pm/ $\mu\epsilon$  and  $\sim 1.4$  pm/ $\mu\epsilon$ , were recorded for the FBGs fabricated in May 2020 and May 2019, respectively.

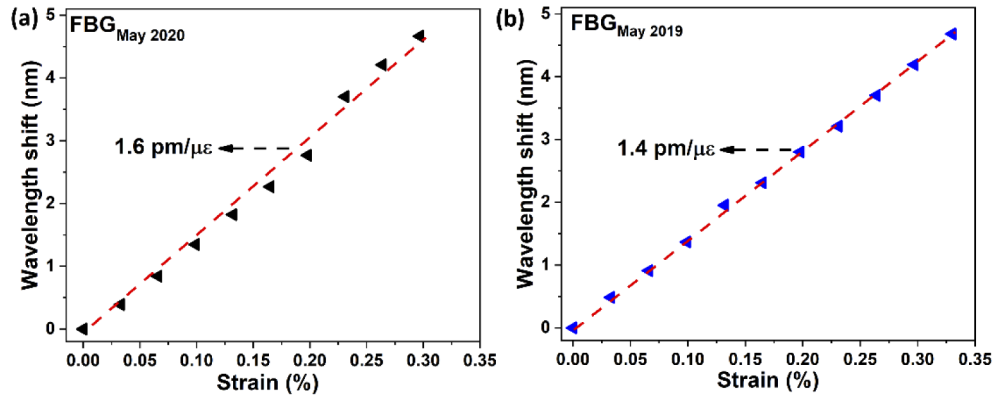


**Fig. 7.** Comparison of strain responses of the FBGs fabricated in (a) May 2020 and (b) May 2019. Both FBGs were inscribed in the same batch of ZEONEX POF drawn in May 2019.

### 3.2. Long-term stability of the fabricated FBG based on SMPOFs

To determine the long-term impact of the irradiated UV wavelength on the strength of the FBG, comparative experiments were conducted using two different UV lasers, namely, 248 nm KrF excimer laser and 325 nm He-Cd laser. The FBGs were fabricated in May 2019, under two pulses of 248 nm laser irradiation and 5 min of 325 nm laser irradiation. The strain responses of these POFBGs were explored in May 2020. In an attempt to introduce an elongation to the FBG under investigation, the two ends of the optical fiber with an FBG were fixed onto two 3-axis positioning stages (Thorlabs MAX 350/M) where one of the stages was moved while the other remained stable. The FBGs were elongated manually by 10  $\mu\text{m}$  per step, up to a strain value of  $\sim 0.35\%$ , which is sufficient for vital signs detection of a human body. The results obtained are shown in Fig. 8. After three strain cycles, evidently, a similar response in strain is observed for the FBGs inscribed with the two types of lasers in ZEONEX SMPOF.

Through this comparative study of FBGs inscribed within a time span of one year, it is evident that the POFBGs demonstrate consistency and excellent long-term stability in terms of temperature and strain responses which is key to their potential use in biomedical applications. Furthermore, the similarity in the strain response of the FBGs fabricated more than a year ago using two different types of lasers namely, 325 nm He-Cd laser and 248 nm KrF excimer laser highlight that FBG inscription in SMPOFs using the latter is preferred due to its enhanced fabrication efficiency.

### 3.3. Single pulse production of FBGs in SMPOFs

The ability of fabricating an FBG with a single laser pulse, which allow FBGs to be inscribed during fiber drawing, is an important step towards the mass producibility of low cost FBGs. Figure 9 shows the spectrum of an FBG fabricated with a single pulse with a pulse energy and pulse duration of 65 mJ and 25 ns, respectively. The spectrum was recorded by the Micron optical interrogator (MOI Si155) and the 3 dB bandwidth of the 5 mm grating is  $\sim 0.2$  nm. The

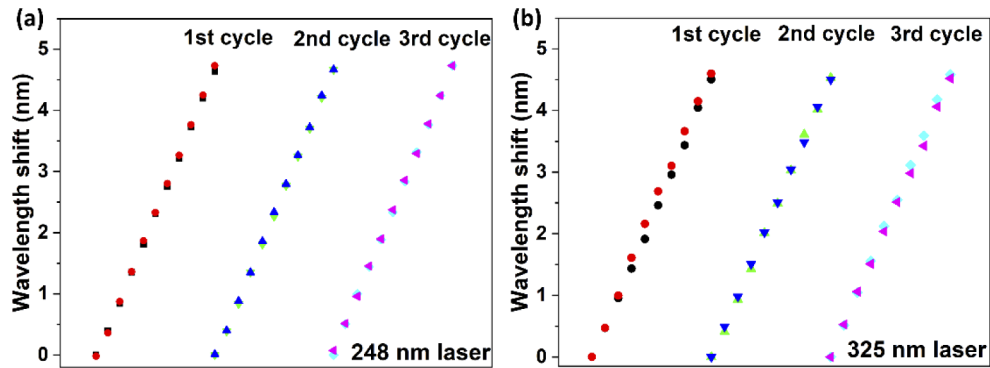


**Fig. 8.** Comparison of strain responses of two FBGs inscribed with (a) 248 nm and (b) 325 nm laser irradiation during three elongation-compress cycles under a 0.35% strain scale. Black and red arrows represent strain loading and unloading conditions, respectively. Both FBGs were inscribed in May 2019 in the same batch of ZEONEX POF.

quality of the FBG is sufficient for sensing applications. This unprecedented fabrication of FBGs in ZEONEX SMPOFs using 248 nm excimer laser irradiation with a single pulse greatly benefits the efficiency of FBG fabrication in POFs and hence, can be useful for cost effective bulk production of FBGs.

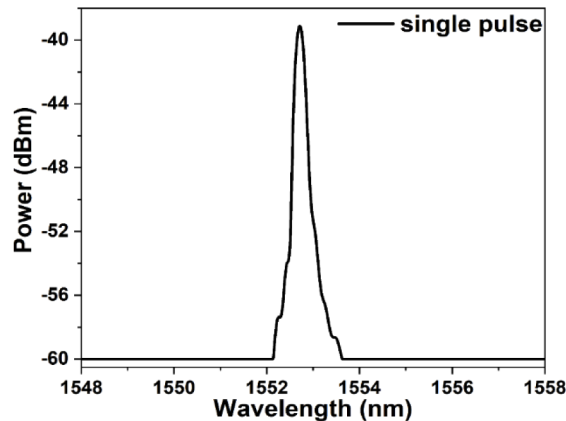


**Fig. 9.** Reflection spectrum profile of a 5 mm long FBG fabricated in ZEONEX SMPOF using a 248 nm excimer laser with a single 25 ns pulse with a pulse energy of 65 mJ.

#### 4. Biomedical applications of ZEONEX SMPOFs

The main potential application area of the proposed ZEONEX-based SMPOF is in biomedical in which POFs inscribed with FBGs can be incorporated in sensing numerous parameters such as temperature, strain, pressure, pH, humidity and vital signs [6,7,9,20–22]. An FBG inscribed in diphenyl disulphide doped SMPOF based on polymethyl methacrylate was employed in our previous reported research study to monitor the heart beat and respiration where sensitivities with an improvement of ~ 20 times and ~ 60 times, respectively were achieved compared to that of FBGs in silica glass fiber [2]. In the current study, silicone rubber was used as a substrate in which the ZEONEX-based POFBG was embedded to monitor multiple vital signs including heart and respiration rates.



The numerous intrinsic features such as low Young's modulus of  $\sim 0.9$  MPa, flexibility and the capacity to attach to human skin surface without the need for any other additional adhesive substances together with excellent biocompatibility [23], makes silicone rubber the preferred choice for the substrate in this study. The mold which was used to fabricate the substrate was 3D printed and the dimensions of the silicone rubber substrate can be altered based on the criteria of the specific application. The ZEONEX-based POFBG was embedded in the substrate to form a sensing device which can be bent and placed on the wrist, chest and abdomen area of an individual in order to detect heart and respiration rates without the use of any adhesive when attaching the sensor to the location of interest.

Figure 10 illustrates the schematic experimental setup used to conduct the measurements and the sensing locations of interest.

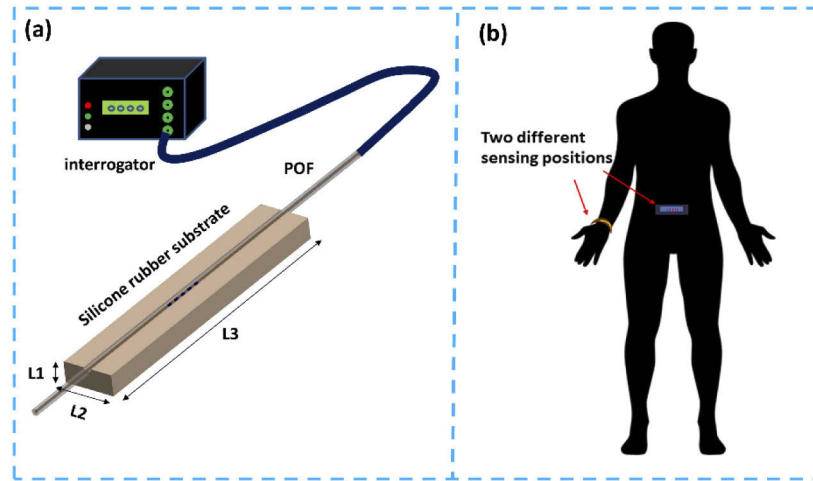


**Fig. 10.** (a) Schematic illustration of the sensing setup; (b) two different sensing localities including wrist and the abdomen.

The sensing device placed on the wrist helps in the detection of the heart rate as shown in Figs. 11(a) and (b), and the other placed on the abdomen aids in sensing the respiration response as shown in Fig. 11(c). The sensing devices used in the two measurements mentioned above, consist of two different dimensions of 1 mm(L1) $\times$ 5 mm(L2) $\times$ 70 mm(L3) which was placed on the wrist, Fig. 11(d), and 1 mm $\times$ 20 mm $\times$ 20 mm which was placed on the abdomen, Fig. 11(e), respectively.

As shown in Fig. 11(b), (a) wavelength amplitude of  $\sim 4$  pm is observed during the measurement of the heart rate, which is 4 times higher compared to that of a silica-based sensor [24]. Furthermore, according to Fig. 11(c) a respiration rate of 21 bpm is recorded for the individual who was subjected to the test where the sensor demonstrates its ability to identify and distinguish inhalation and exhalation while the breath is being held. Moreover, the sensing devices can also benefit from the excellent flexibility of the elongated and square prototypes of the silicone rubber substrates shown in Figs. 11(f) and (g), respectively, which aids to attach the sensor onto the surface of the skin at different localities of the human body.

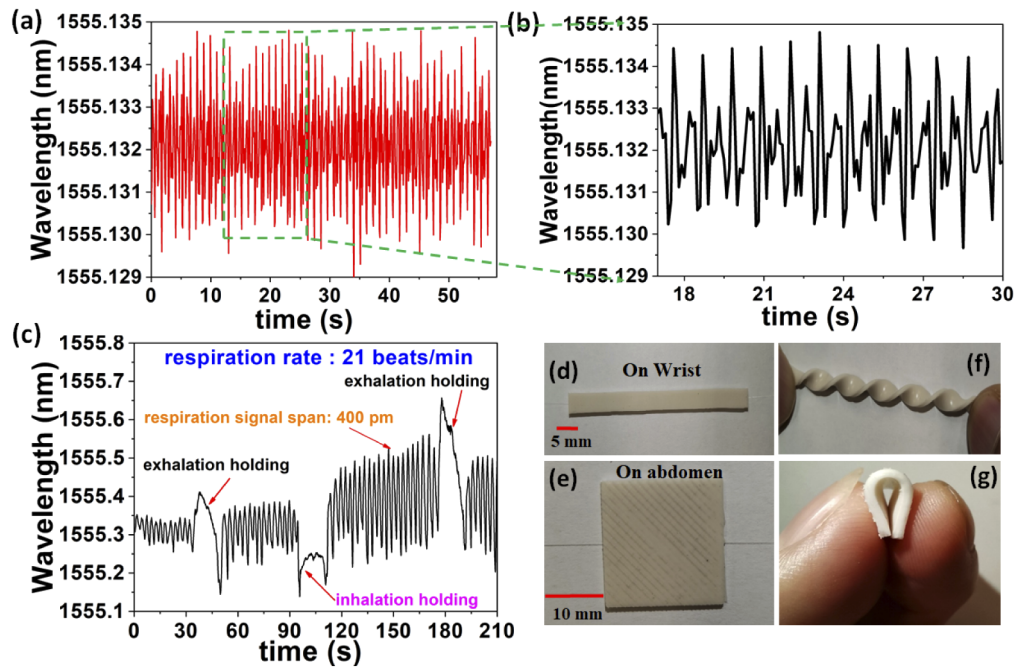


**Fig. 11.** FBG waveforms generated during the detection of (a) heart rate; (b) its expanded view; (c) respiration rate with the sensing devices placed on the (d) wrist and (e) abdomen and indication of the flexibility of the sensing devices placed on the (f) wrist and the (g) abdomen.

## 5. Conclusion

In summary, we report for the first time, POFBGs fabricated with a single pulse of 25 ns 248 nm UV laser irradiation in solely ZEONEX based POFs, where the core and cladding consists of a single material. This approach can significantly enhance the POFBG fabrication procedure at 1550 nm wavelength range to produce consistent and good quality FBG sensors and further encourages mass production of FBGs during the fiber drawing process with reduced production costs. Furthermore, characterizations conducted on the ZEONEX-based SMPOF outline the influence of O<sub>2</sub> during the fiber fabrication process. Exploration of physical parameters such as temperature and strain over a time frame of one year together with performance comparisons with respect to 325 nm laser irradiated POFBGs, emphasize the long-term feasibility of these 248 nm laser irradiated POFBGs. In addition, a sensing device comprising of a silicone rubber substrate embedded with POFBGs is proposed for heart rate and respiration measurements where a commendable performance is observed in the detection of these vital signs. Moreover, the sensing device also exhibits its capability to distinguish inhalation and exhalation while the breath is held. The intrinsic properties of ZEONEX material such as low Young's modulus, affinity to water and good chemical inertness to bases, acids, and many polar solvents revitalize fiber optic research on SMPOFs which are ideal for medical sensing systems including in vivo measurements.

## Funding

The Hong Kong Polytechnic University (1-ZVGB); Research Grants Council, University Grants Committee (PolyU 152087/18E).

## Disclosures

The authors declare no conflict of interest.

## References

1. S. Koyama and H. Ishizawa, "Vital Sign Measurement Using FBG Sensor for New Wearable Sensor Development," in *Fiber Optic Sensing - Principle, Measurement and Applications* (IntechOpen, 2019).
2. J. Bonefacino, H.-Y. Tam, T. S. Glen, X. Cheng, C.-F. J. Pun, J. Wang, P.-H. Lee, M.-L. V. Tse, and S. T. Boles, "Ultra-fast polymer optical fibre Bragg grating inscription for medical devices," *Light: Sci. Appl.* **7**(3), 17161 (2018).
3. M. Fajkus, J. Nedoma, R. Martinek, V. Vasinek, H. Nazeran, and P. Siska, "A non-invasive multichannel hybrid fiber-optic sensor system for vital sign monitoring," *Sensors* **17**(12), 111–117 (2017).
4. Y. Haseda, J. Bonefacino, H. Y. Tam, S. Chino, S. Koyama, and H. Ishizawa, "Measurement of pulse wave signals and blood pressure by a plastic optical fiber FBG sensor," *Sensors* **19**(23), 5088 (2019).
5. H.-Y. Tam, Z. Liu, D. S. Gunawardena, A. N. Vadivelu, B. Chen, D. Oetomo, and S. O'Leary, "Sixth International Workshop on Specialty Optical Fibers and Their Applications (WSOF 2019): Conference Digest," in *Sixth International Workshop on Specialty Optical Fibers and Their Applications (WSOF 2019)* (SPIE, 2019), 1120601 (November 2019).
6. J. Bonefacino, X. Cheng, C.-F. J. Pun, S. T. Boles, and H.-Y. Tam, "Impact of high UV fluences on the mechanical and sensing properties of polymer optical fibers for high strain measurements," *Opt. Express* **28**(2), 1158 (2020).
7. A. G. Leal-Junior, C. A. R. Diaz, L. M. Avellar, M. J. Pontes, C. Marques, and A. Frizera, "Polymer Optical Fiber Sensors in Healthcare Applications: A Comprehensive Review," *Sensors* **19**(14), 3156 (2019).
8. D. J. Webb, "Fibre Bragg grating sensors in polymer optical fibres," *Meas. Sci. Technol.* **26**(9), 092004 (2015).
9. X. Cheng, J. Bonefacino, B. O. Guan, and H. Y. Tam, "All-polymer fiber-optic pH sensor," *Opt. Express* **26**(11), 14610–14616 (2018).
10. C. Wochnowski, S. Metev, and G. Sepold, "UV-laser-assisted modification of the optical properties of polymethylmethacrylate," *Appl. Surf. Sci.* **154–155**, 706–711 (2000).
11. A. Pospori, C. A. F. Marques, O. Bang, D. J. Webb, and P. André, "Polymer optical fiber Bragg grating inscription with a single UV laser pulse," *Opt. Express* **25**(8), 9028 (2017).
12. A. Stefani, W. Yuan, C. Markos, and O. Bang, "Narrow bandwidth 850-nm fiber Bragg gratings in few-mode polymer optical fibers," *IEEE Photonics Technol. Lett.* **23**(10), 660–662 (2011).
13. W. Yuan, L. Khan, D. J. Webb, K. Kalli, H. K. Rasmussen, A. Stefani, and O. Bang, "Humidity insensitive TOPAS polymer fiber Bragg grating sensor," *Opt. Express* **19**(20), 19731–9 (2011).
14. G. Woyessa, A. Fasano, A. Stefani, C. Markos, K. Nielsen, H. K. Rasmussen, and O. Bang, "Single mode step-index polymer optical fiber for humidity insensitive high temperature fiber Bragg grating sensors," *Opt. Express* **24**(2), 1253 (2016).
15. O. Bang, C. Markos, K. Nielsen, A. Stefani, W. Yuan, and H. K. Rasmussen, "High-Tg TOPAS microstructured polymer optical fiber for fiber Bragg grating strain sensing at 110 degrees," *Opt. Express* **21**(4), 4758 (2013).
16. G. Woyessa, A. Fasano, C. Markos, A. Stefani, H. K. Rasmussen, and O. Bang, "Zeonex microstructured polymer optical fiber: fabrication friendly fibers for high temperature and humidity insensitive Bragg grating sensing," *Opt. Mater. Express* **7**(1), 286 (2017).
17. G. Woyessa, H. K. Rasmussen, and O. Bang, "Zeonex – a route towards low loss humidity insensitive single-mode step-index polymer optical fiber," *Opt. Fiber Technol.* **57**(April), 102231 (2020).
18. Zeon, "Cyclo Olefin Polymer New high-performance thermoplastics for next-generation," ZEON Corp. 59, (2018).
19. A. N. Vadivelu, Z. Liu, D. S. Gunawardena, B. Chen, H. Y. Tam, S. O'Leary, and D. Oetomo, "Integrated Force Sensor in a Cochlear Implant for Hearing Preservation Surgery," in *Proceedings of the Annual International Conference of the IEEE Engineering in Medicine and Biology Society, EMBS* (IEEE, 2019), pp. 3819–3822.
20. A. Leal-Junior, A. Frizera-Netoc, C. Marques, and M. J. Pontes, "A polymer optical fiber temperature sensor based on material features," *Sensors* **18**(2), 301 (2018).
21. X. Cheng, Y. Liu, and C. Yu, "Gas pressure sensor based on BDK-doped polymer optical fiber," *Micromachines* **10**(11), 717 (2019).
22. A. G. Leal-Junior, C. R. Díaz, M. J. Pontes, C. Marques, and A. Frizera, "Polymer optical fiber-embedded, 3D-printed instrumented support for microclimate and human-robot interaction forces assessment," *Opt. Laser Technol.* **112**(October 2018), 323–331 (2019).
23. P. V. Mohanan and K. Rathinam, "Biocompatibility studies on silicone rubber," in *IEEE/Engineering in Medicine and Biology Society Annual Conference* (1995), pp. 11–12.
24. Y. Katsuragawa and H. Ishizawa, "Non-invasive blood pressure measurement by pulse wave analysis using FBG sensor," *2015 IEEE Int. Instrum. Meas. Technol. Conf. Proc.* 511–515 (2015).